1 Supplementary Information

The work presented here is a demonstration of the depth inspection capability of lock-in thermography; as well established for other, non-fuel cell, applications [1-3]. Figure A1(a) shows an exploded view of the experiment, constructed of FR4 layers. The validation looks at how varying the lock-in frequency allows an object to be analysed by slices (varying depth 'focus'), complementing the approximate penetration depth calculation given in Equation 1 of the main text.

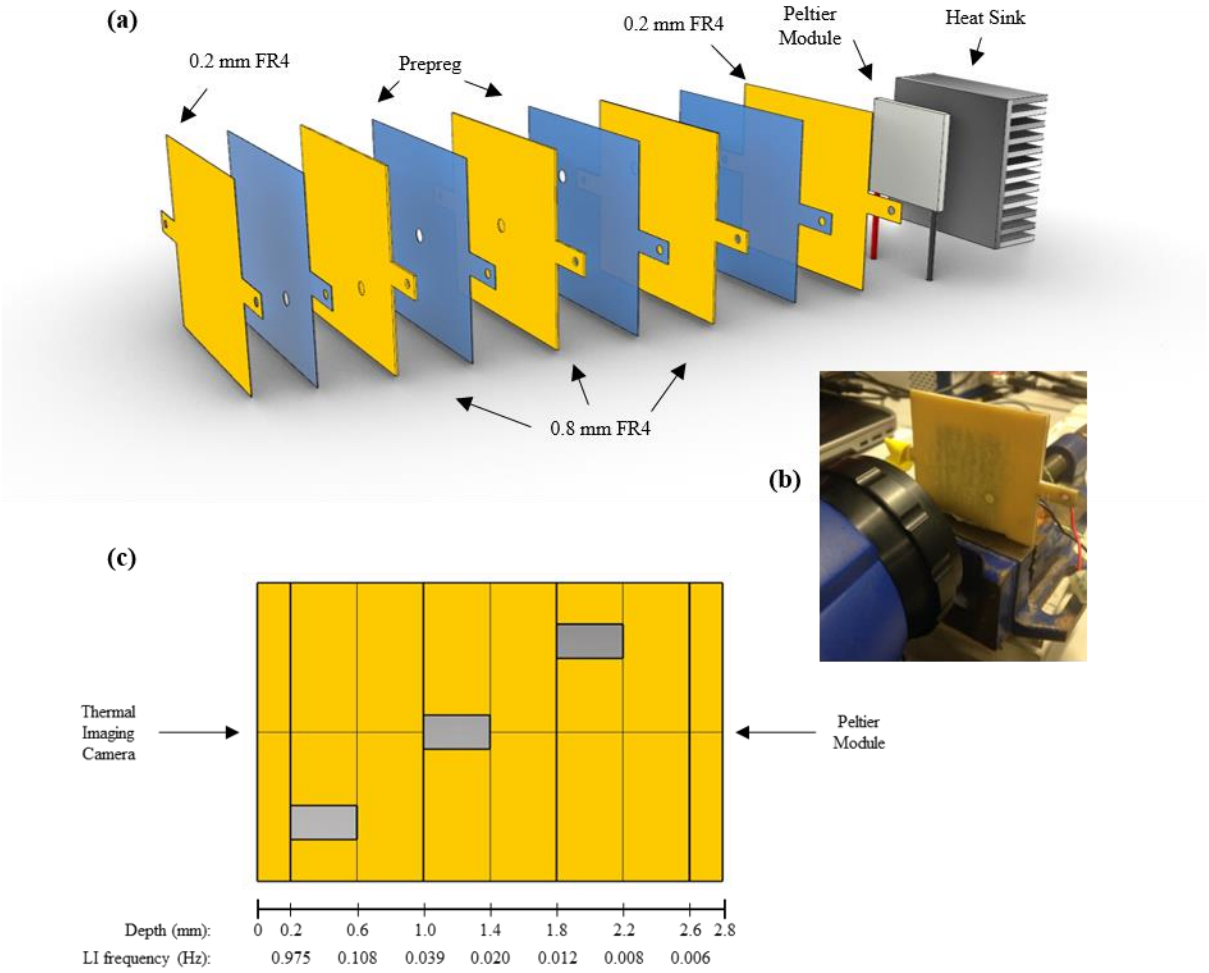

Figure A1: (a) 'Exploded' view of the depth inspection experiment showing the layers as they would be before hot-pressing together. The Peltier module is attached to the back plate and the thermal imaging camera is pointed at the front plate. (b) Photograph of the experimental setup with the bottom right circle visible. (c) Inspection depths and approximate lock-in detection frequencies for the different layers.

The same Peltier module was operated as in the lock-in experiment for comparable analysis. There are three 0.8 mm thick FR4 plates with 0.4 mm deep, 5 mm diameter circles milled out of them at different spatial locations, illustrated in Figure A1(c). 0.2 mm FR4 sheets sandwich the composition, emulating the endplates of the fuel cell. Prepreg layers bind each layer together, with the hot-pressing technique outlined in the main paper. The lock-in perturbation frequency was investigated between 0.004 and 0.07 Hz with a 1 Hz PWM frequency. Frequencies higher than 0.07 Hz were not investigated, as reaching steady thermal equilibrium was not possible with the Peltier module.

The lock-in signal sent to the camera and the recorded thermal perturbation imposed on the exhibited a small time delay, shown in Figure A2. These were synchronised prior to the lock-in acquisition.

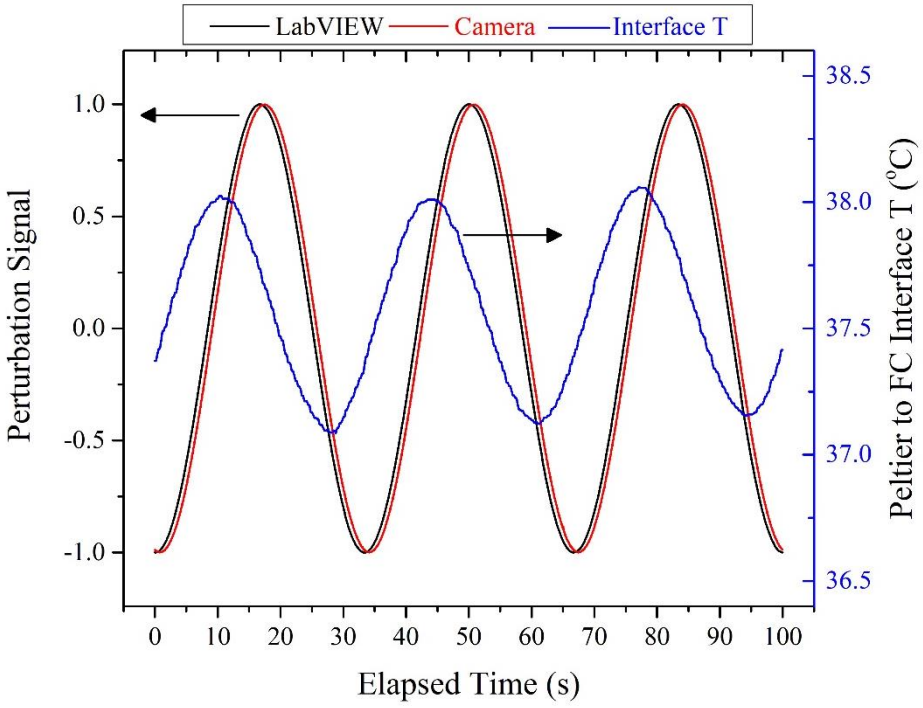

Figure A2: Observation of recorded 0.03 Hz perturbation signal from the LabVIEW software, received by the thermal camera and the heating and cooling imposed on the PEFC by the Peltier module.

Figure A3 shows the selected lock-in phase images generated for perturbation frequencies of 0.07, 0.03, 0.009, 0.006 and 0.004 Hz. These correspond to approximate penetration depths of 0.75, 1.14, 2.08, 2.55 and 3.12 mm from the surface facing the thermal camera. Cross-

correlation peak profiles were created for each image by drawing a diagonal line profile from the top left to bottom right corner, normalised and plotted in Figure A4.

A discernible trend of decreasing overall phase shift is detected with longer excitation periods. This is due to the reduced attenuation of the thermal wave through the sample, reiterated by the reduction in noisy data. It should be noted that the figure legends are not fixed in Figure A3 due to the large range of phase values, so the false-image colour should not be compared per image but rather the magnitude and phase contrast.

The bottom right circle is not detected in any of the phase images, which suggests that higher frequencies are required to image it, in accordance with the penetration depth equation. In general, the phase contrast of the other two holes is higher than the surrounding FR4, due to the presence of air inside the voids, which is 10 times less thermally conductive [4]. The central and top left circle is visible in every image, but at varying intensities.

The rough location of the central circle is expected at 0.03 Hz, and here it has the greatest contrast with the surrounding FR4 body and visible top left circle, as evident by the peak in the normalised image. Decreasing frequency sees the detection depth move further into the sample as proven by the signal reduction for the central circle in contrast to the surrounding FR4 and a narrowing of the normalised peak.

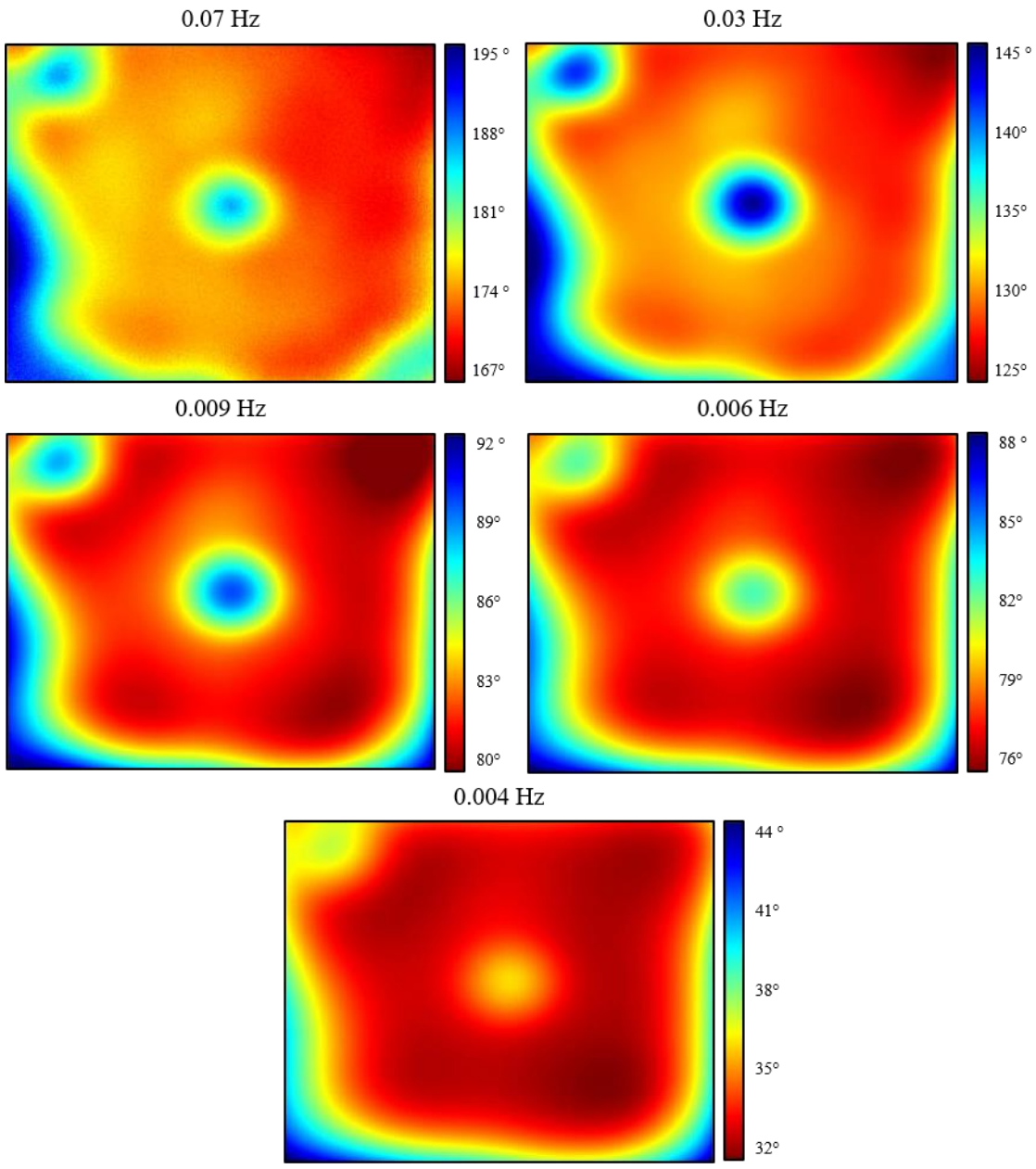

Figure A3: Lock-in phase images at different perturbation frequencies with varying legend range.

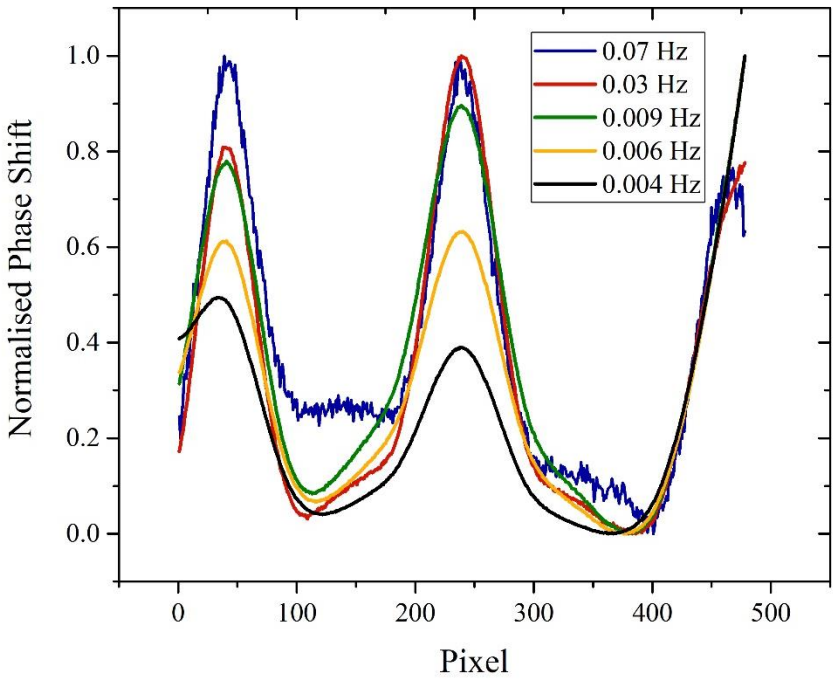

Figure A4: Normalised phase shift results of the line profile that passes through each circle at different lock-in frequencies.

Contrarily, decreasing frequency features an increase in signal for the top left circle, but it is only until 0.004 Hz that the normalised phase shift peak of the top left circle surpasses the middle circle. Interestingly, these results were expected at 0.009 Hz, which is the depth location of the top left circle. A perturbation frequency of 0.004 Hz should correspond to a penetration depth greater than the sample thickness. It is clear that the penetration depth equation has a degree of inaccuracy, but this is expected as lateral heating has not been taken into consideration.

The effects of lateral heating and Peltier edge effects is exhibited in the corners of the phase images, exacerbated for lower frequencies, shown in the steep normalised values on the bottom right corner. This had been corrected for in the fuel cell experiments in the report by ensuring the imaging view was within the Peltier heating domain.

What is evident however, is that the lock-in thermography diagnostic tool can be used as a depth perception tool, proven by the gradual change in peaks of the three circles for changing perturbation frequency and the penetration depth equation can be used as an approximation to select these appropriate frequencies.

2 References

1. Mulaveesala, R. and S. Tuli, *Theory of frequency modulated thermal wave imaging for nondestructive subsurface defect detection.* Applied Physics Letters, 2006. **89**(19): p. 191913.
2. Schmidt, C., et al. *Application of lock-in thermography for 3d defect localisation in complex devices*. in *2008 2nd Electronics System-Integration Technology Conference*. 2008.
3. Robinson, J.B., et al., *Detection of internal defects in lithium-ion batteries using lock-in thermography.* ECS Electrochemistry Letters, 2015. **4**(9): p. A106-A109.
4. Clyde F. Coombs, Jr., *Current Carrying Capacity in Printed Circuits*, in *Printed Circuits Handbook, Sixth Edition*. 2008, McGraw Hill Professional, Access Engineering.